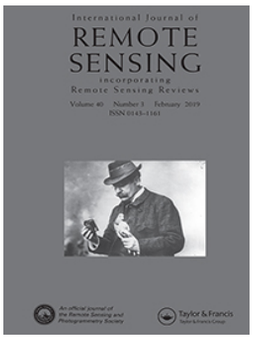

International Journal of Remote Sensing

ISSN: 0143-1161 (Print) 1366-5901 (Online) Journal homepage: https://www.tandfonline.com/loi/tres20

Identifying local anthropogenic CO_2 emissions with satellite retrievals: a case study in South Korea

Changsub Shim, Jihyun Han, Daven K. Henze & Taeyeon Yoon

To cite this article: Changsub Shim, Jihyun Han, Daven K. Henze & Taeyeon Yoon (2019) Identifying local anthropogenic CO_2 emissions with satellite retrievals: a case study in South Korea, International Journal of Remote Sensing, 40:3, 1011-1029, DOI: 10.1080/01431161.2018.1523585

To link to this article: https://doi.org/10.1080/01431161.2018.1523585

Published online: 11 Oct 2018.

INTERNATIONAL JOURNAL OF REMOTE SENSING
2019, VOL. 40, NO. 3, 1011–1029
https://doi.org/10.1080/01431161.2018.1523585

Taylor & Francis
Taylor & Francis Group

Identifying local anthropogenic CO_2 emissions with satellite retrievals: a case study in South Korea

Changsub Shim [a], Jihyun Han[a], Daven K. Henze[b] and Taeyeon Yoon[c]

[a]Korea Environment Institute, Sejong, South Korea; [b]University of Colorado, Boulder, CO, USA; [c]Sunmoon University, Chungcheonnam-do, South Korea

ABSTRACT

We used multiyear Greenhouse Gases Observing Satellite (GOSAT) dry air, column-integrated CO_2 (XCO_2) retrievals (2010–2013) to evaluate urban and local-scale CO_2 emissions over East Asia and examined whether GOSAT XCO_2 captures the impact of strong local CO_2 emissions over South Korea, an East Asian downwind region with high atmospheric aerosol loading and strong summer monsoons. We chose a region in western Mongolia (upwind region) as the XCO_2 background, and estimated XCO_2 enhancements in South Korea to gauge local and regional emissions. We found that the cold season (November–February) was better suited for estimating XCO_2 enhancements of local emissions due to the summer monsoon and stronger transboundary impacts in other seasons. In particular, we focused on three local GOSAT XCO_2 footprints (about 10.5 km in diameter) in South Korea: the Seoul Metropolitan Area (SMA), the Gwangyang Steelworks and Hadong power plants (GYG), and the Samcheonpo power plants (SCH). The range of XCO_2 enhancement was 7.3–10.7 ppm (14.1–21.3 mg m^{-3} in standard temperature and pressure (STP)). By estimating other important contributions to XCO_2 enhancements such as the XCO_2 latitudinal gradients and Chinese fossil fuel combustions, we estimated the net enhancements caused mainly by local CO_2 emissions in the range of 4.2–7.6 ppm (8.1–14.7 mg m^{-3} in STP) These high enhancements imply that large point source contributions are an important factor in determining these enhancements, even if contributions are also made by broader-scale emissions. Additionally, differences in net XCO_2 enhancements and trends between GYG (+ 4.2 ppm (+ 8.2 mg m^{-3} in STP), – 0.2 ppm $year^{-1}$ (–0.4 mg m^{-3} $year^{-1}$ in STP)) and SCH (+ 7.6 ppm (+ 14.9 mg m^{-3} in STP), + 1.3 ppm $year^{-1}$ (+ 2.6 mg· m^{-3} $year^{-1}$ in STP)) indicate that these closely located footprints (approximately 26 km apart) are separable. These results will be useful in evaluating and reducing uncertainties in regional and local anthropogenic greenhouse gas (GHG) emissions over East Asia.

ARTICLE HISTORY
Received 27 December 2017
Accepted 28 August 2018

1. Introduction

Carbon dioxide (CO_2) is the most important greenhouse gas (GHG), and a large increase in anthropogenic CO_2 emissions has been considered a main driver of global climate change (IPCC 2014). Currently, the world's largest CO_2 emissions are from East Asia

CONTACT Changsub Shim marchell@gmail.com Korea Environment Institute, Sejong, South Korea

(Boden et al. 2010); the top-ranked CO_2-emitting nations are China (1st), Japan (4th), and South Korea (7th). However, there are large uncertainties in CO_2 emission inventories, mainly because of imperfections in bottom-up energy statistics and a lack of observations for validating CO_2 fluxes, particularly over China (Guan et al. 2012; Liu et al. 2015b). These shortcomings lead to critical uncertainty in understanding the link between the global carbon budget and climate change (Guan et al. 2012).

Satellite observations of atmospheric CO_2 have been widely used to monitor atmospheric CO_2 concentrations in the 21st century (Burrows et al. 1995; Bovensmann et al. 1999; Crisp et al. 2004; Engelen and Stephens 2004, 2004; Chevallier et al. 2005; Crevoisier et al. 2009; Kuze et al. 2009; Kulawik et al. 2010), and have contributed to top-down flux estimates of GHGs (Ciais et al. 2010; Chevallier et al. 2014; Deng et al. 2014; Liu et al. 2014; Reuter et al. 2014; Deng et al. 2015). However, CO_2 detection from space has limitations, partly due to the interference of atmospheric clouds and aerosols (Kuze et al. 2009; Crisp et al. 2012; Kort et al. 2012; O'Dell et al. 2012; Zhang, Jiang, and Zhang 2015), resulting in the collection of less data during the wet season and when aerosol loadings in the atmosphere are high.

The Greenhouse Gases Observing Satellite (GOSAT) is a satellite instrument that provides XCO_2-containing information of surface CO_2 fluxes (Yokota et al. 2009). There have been efforts to estimate surface CO_2 fluxes with XCO_2 at a subcontinental scale (Liu et al. 2014; Deng et al. 2015), but low signal sensitivity and sparse sampling of GOSAT XCO_2 are limitations for inferring smaller-scale (urban/local) CO_2 flux information (National Research Council (NRC) 2010; Keppel-Aleks, Wennberg, and Schneider 2011; Ciais et al. 2015).

Despite spatial limitations on inferring CO_2 fluxes with XCO_2, strong CO_2 emissions from megacities create localized CO_2 domes, overwhelming the influence of the urban biosphere (Pataki et al. 2007; Rigby et al. 2008; Newman et al. 2013). Kort et al. (2012) demonstrated XCO_2 enhancement over the Los Angeles Basin, USA, using GOSAT data in the context of urban-scale emissions.

We attempted to assess local CO_2 emissions in South Korea, a downwind region in East Asia, using GOSAT XCO_2. The uncertainty of the South Korea CO_2 emissions inventory is relatively high (Asefi-Najafabady et al. 2014). The most challenging part of this study is the paucity of XCO_2 data due to persistent and high atmospheric aerosol concentrations and extensive cloud cover during the Asian summer monsoon. Additionally, the strong influence of CO_2 outflow from China makes it difficult to evaluate local emissions over downwind regions using XCO_2 retrievals. Despite these limitations, long-term GOSAT XCO_2 observations since 2009 have provided recurrent data over the emission area. Strong XCO_2 enhancements above the background XCO_2 level could help gauge the relationship between XCO_2 concentrations and local CO_2 emissions.

The main objective of this study was to examine whether the impact of strong CO_2 emissions can be captured by satellite XCO_2 retrieval in an East Asian downwind region. As a case study, we used retrievals over South Korea, a highly and extensively polluted region under strong climatological variation. Defining the most appropriate season for evaluating anthropogenic XCO_2 signals and determining the background region to evaluate XCO_2 enhancements over East Asia were also important objectives of this study.

2. Data and study region

2.1. *GOSAT XCO_2 data*

GOSAT is the first satellite instrument designed specifically to measure atmospheric CO_2 and methane concentrations with good sensitivity near the Earth's surface. GOSAT has a 666 km sun-synchronous orbit and completes one orbit in approximately 100 min, providing global sampling in approximately 3 days (Kadygrov et al. 2009). The GOSAT Thermal And Near-infrared Sensor for carbon Observation (TANSO) comprises the Fourier Transform Spectrometer (FTS) and the Cloud Aerosol Imager (CAI) (Kuze et al. 2009). The TANSO-FTS has three bands in the shortwave infrared (SWIR) region (0.8, 1.6, and 2.0 μm) and a wide thermal infrared (TIR) band (5.5–14.3 μm) with a circular instantaneous footprint of approximately 10.5 km at the nadir (Yokota et al. 2009). The retrieval of greenhouse gases from FTS spectra excludes cloudy pixels by screening the images from CAI, resulting in significant data reduction (Kadygrov et al. 2009).

We used XCO_2 (v3.3, level 2) retrieved by Atmospheric CO_2 Observations from Space retrievals from GOSAT (ACOS-GOSAT) via the National Aeronautics and Space Administration (NASA 2018) Goddard Earth Science Data and Information Services Center for April 2009 to April 2013. We removed low-quality data using a master quality flag that defines retrieval success by cloud screening and retrieval algorithm diagnostics. The retrieval method and data products have been described in previous studies (Wunch et al. 2011; Crisp et al. 2012; O'Dell et al. 2012).

2.2. *Study regions*

The ACOS GOSAT XCO_2 retrieval algorithm excluded data with high aerosol optical depth and cloud optical thickness (Crisp et al. 2012; O'Dell et al. 2012), resulting in less XCO_2 data over East Asia during the Asian summer monsoon (Kort et al. 2012) and high pollution events, which typically occur in the spring (not shown).

Figure 1 shows the East Asian regions with GOSAT monthly mean XCO_2 concentrations in February 2010; a GOSAT overpass over the Korean peninsula is shown in Figure 2. We focused on the three GOSAT footprints with the highest frequency for the 4 years of data (>30 retrievals between April 2009 and April 2013): the Seoul Metropolitan Area (SMA), the Gwangyang Steelworks and Hadong coal power plants (GYG), and the Samcheonpo coal power plants (SCH) (Figure 3).

GOSAT XCO_2 over SMA is located near central SMA, where the CO_2 emission intensity was 140 kg m^{-2} $year^{-1}$ based on a fossil fuel data assimilation system (FFDAS v2.0, Asefi-Najafabady et al. 2014) with a $0.1° \times 0.1°$ spatial resolution in 2010. However, XCO_2 over the SMA footprint (127.011°E, 37.603°N) can be influenced by the entire SMA region (Figure 3) from diverse emission sources (e.g., transportation and household; National Research Council (NRC) 2010).

The emissions over GYG and SCH indicate more specific local sources (Figure 3). The GOSAT footprint over GYG (127.854°E, 35.012°N) included the Hadong coal power plants and Gwangyang Steelworks, which are located within 10 km of the centre of the GYG footprint (Figure 3). The SCH footprint (128.14°E, 34.99°N) is adjacent to the Samcheonpo coal power plants (within approximately 7 km of the centre of SCH). The

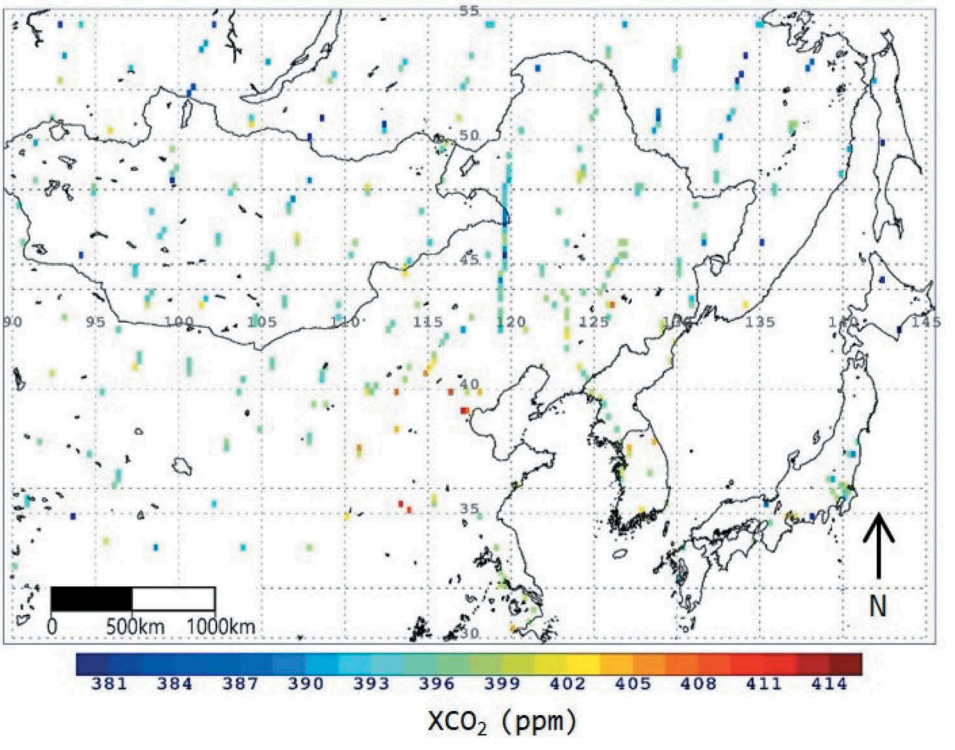

Figure 1. The spatial coverage of GOSAT XCO_2 data (version 3.3, Nadir mode only) in February 2012. The colour denotes XCO_2 concentration (ppm).

emission intensities of GYG and SCH were 308 kg m^{-2} $year^{-1}$ and 270 kg m^{-2} $year^{-1}$, respectively; these were not significantly affected by other nearby major emission sources.

Gwangyang Steelworks is the largest steelworks in South Korea, producing more than 2×10^{10} kg $year^{-1}$ of steel products (Kim 2016). The Hadong and Samcheonpo coal power plants are in the largest class of coal power plants in South Korea, each emitting more than 2.5×10^{10}kg of CO_2 per year (KOEN 2016; KOSPO 2016). Thus, the GYG and SCH footprints overpass large local CO_2 point sources in the southern coastal region of South Korea, enabling us to assess the local emission impact on the GOSAT XCO_2.

We did not apply OCO-2 data in this study because the swath does not cover the same locations, and sparse sampling of 'good' retrievals and a shorter observation period yields less data for analysis.

3. Results

3.1. *Background regions*

To estimate XCO_2 enhancements due to large urban/local anthropogenic emissions, a reliable XCO_2 background must be defined. The criteria for the XCO_2 background were as follows:

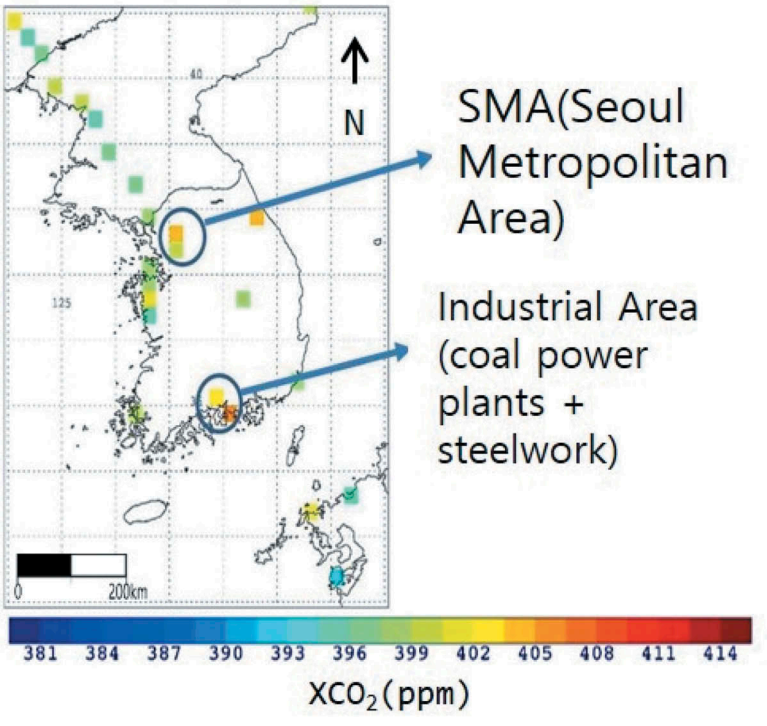

Figure 2. Same as Figure 1, but zoomed in to show the observation overpass over the Korean Peninsula.

- The background region does not include large emissions.
- The background region should be minimally influenced by the transport of CO_2 emissions/sinks.
- The XCO_2 over the background must have higher precision with a large amount of data, and represent typical seasonal trends.

Large and extensive CO_2 emissions over East Asia make it difficult to find 'clean' background regions near the emissions targets (Figure 4) in the manner that Kort et al. (2012) used to define the desert area near The Los Angeles Basin as the background. Thus, we chose two regions for XCO_2 background outside extensive emission regions in East Asia: western Mongolia (95–105°E, 44–49°N) and far eastern Russia (135–145°E, 45–53°N), where there are no noticeable anthropogenic emission sources (Figure 4). Western Mongolia is mainly characterized by grassland and shrubs (steppe) and does not include pollution from the nation's capital (Ulaanbaatar). Far eastern Russia comprises mainly mountainous forests.

Figure 5 shows the monthly variation in XCO_2 over western Mongolia and far eastern Russia with the number of XCO_2 retrievals. These regions displayed an annual trend of + 2.2 ppm $year^{-1}$ and + 1.7 ppm $year^{-1}$, respectively. Far eastern Russia exhibited larger seasonal variability, with higher XCO_2 in spring and lower XCO_2 in summer, indicating the higher influence of emissions from northern China in the spring and strong

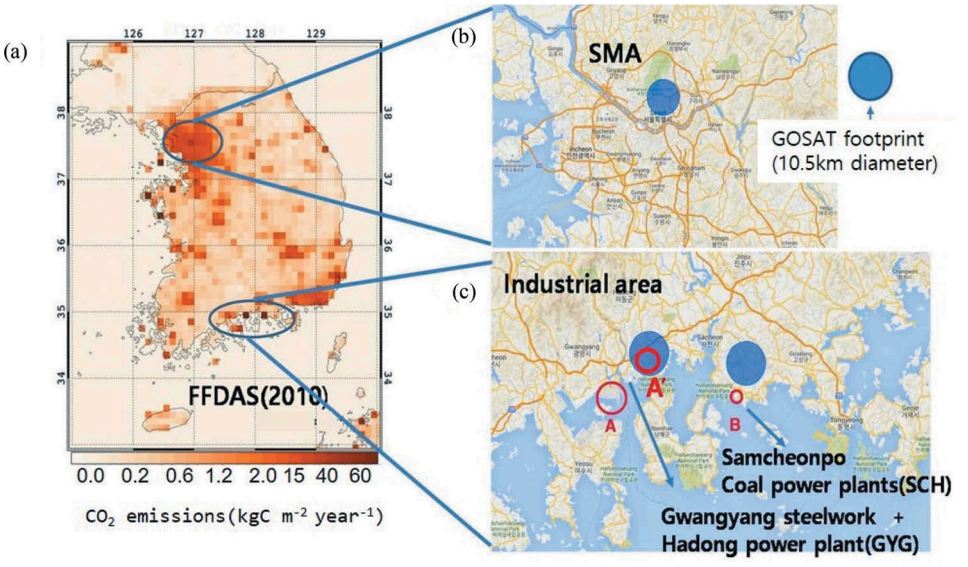

Figure 3. The CO_2 emissions based on FFDAS 2010 inventory (left panel (a) with unit of kgC m^{-2} $year^{-1}$) and geographical identification of the three-selected GOSAT XCO_2 footprints (blue-coloured circles denotes the actual size of GOSAT diameter; right panel). Sungbuk-ku in Seoul Metropolitan Area (SMA) (panel b), Gwangyang Steelwork & Hadong power plants (GYG), and Samcheonpo power plants (SCH) (panel c).

vegetation uptake in summer. Additionally, the monthly sampling mean over far eastern Russia (19) was less than that over western Mongolia (44), leading to poorer precision of monthly mean XCO_2 (± 4.9 ppm vs. ± 3.2 ppm). The stable seasonal trend with higher precision over western Mongolia enabled us to select it as the background for East Asian XCO_2 enhancements.

Therefore, western Mongolia can be used as a background to estimate XCO_2 enhancement over East Asia, including the Korean peninsula.

We did not use XCO_2 values over the ocean (i.e., the Yellow Sea) as a background because GOSAT XCO_2 over ocean is collected using a different observation mode (glint mode), which provides relatively large uncertainty and much lower data density than the nadir mode over land (Liu et al. 2014; Zhou et al. 2016).

Determining the season for which to quantify the background and enhanced XCO_2 is another important process. Higher cloud cover and strong influences of biogenic CO_2 uptake in summer are critical restrictions in this study. In particular, there are large latitudinal XCO_2 gradients over East Asia (30°N–45°N) in summer due to strong CO_2 uptake from northern Asia and Russia, which strongly dilutes the impact of anthropogenic emissions (Shim, Lee, and Wang 2013). Additionally, the stronger impact of long-range transport of CO_2 emissions on measured XCO_2 over far eastern Russia in the spring and fall is associated with less data and higher uncertainty (Figure 5) due to high aerosol concentrations in that season (not shown). Thus, performing analysis in the cold season (November–February) has the advantage of minimizing the influence of biospheric fluxes.

When we consider western Mongolia (upwind) as the XCO_2 background, the influence of latitudinal difference should be taken into account. Although Keppel-

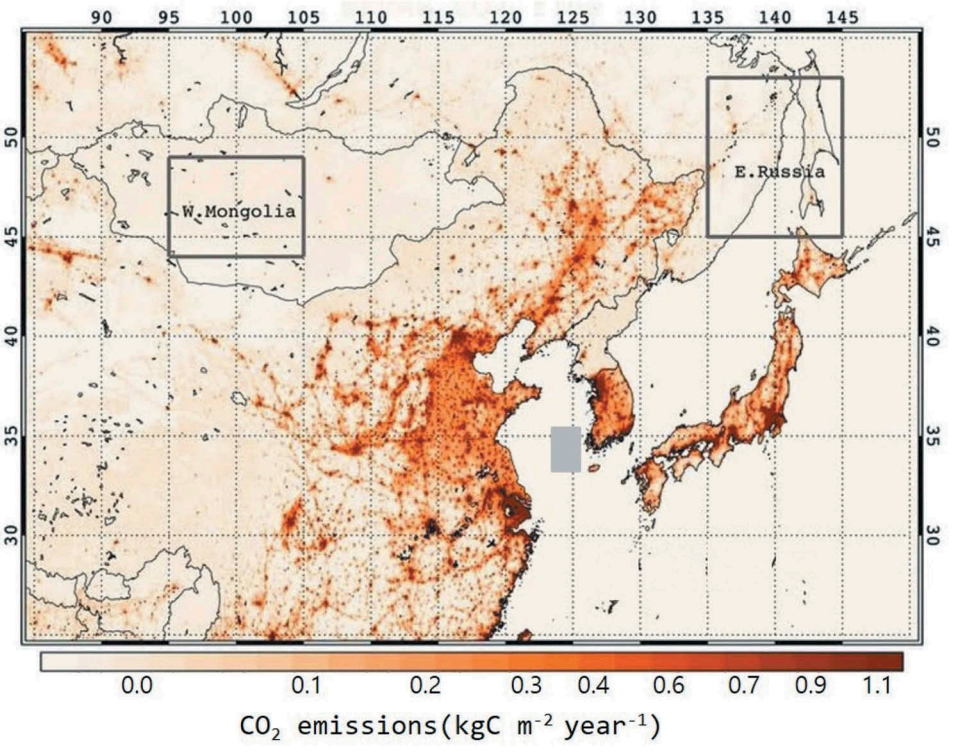

Figure 4. The CO_2 emission strength and distribution over East Asia estimated by FFDAS global anthropogenic CO_2 emission inventory of 2010. The grey region over the Yellow Sea is defined to estimate the contribution to XCO_2 by Chinese fossil fuel combustions with GEOS-Chem model.

Aleks et al. (2013) designated the upwind region of the Asian continent as a background with northern and southern boundaries (35–48°N) based on potential temperature, GOSAT XCO_2 has helped to quantify latitudinal gradients of XCO_2 in East Asia; the difference in XCO_2 between 45° N and 35° is approximately 1.3 ppm. This latitudinal difference of XCO_2 is also supported by Shim, Lee, and Wang (2013) and Eldering et al. (2017).

3.2. *XCO_2 enhancements over large emission sources*

We used the monthly mean GOSAT XCO_2 data because the total number of XCO_2 retrievals within a month is mostly one or two. For higher sample sizes, Kort et al. (2012) demonstrated that there was no statistical difference in XCO_2 among 10 day, 20 day, and 30 day averages for the Los Angeles Basin.

The monthly XCO_2 over the three footprints in South Korea from April 2009 to April 2013 is shown in Figure 6, which compares the enhanced XCO_2 from SMA, GYG, and SCH to that of the background region (western Mongolia). As previously described, some monthly data are missing every summer due to the extensive cloud cover (Figure 6).

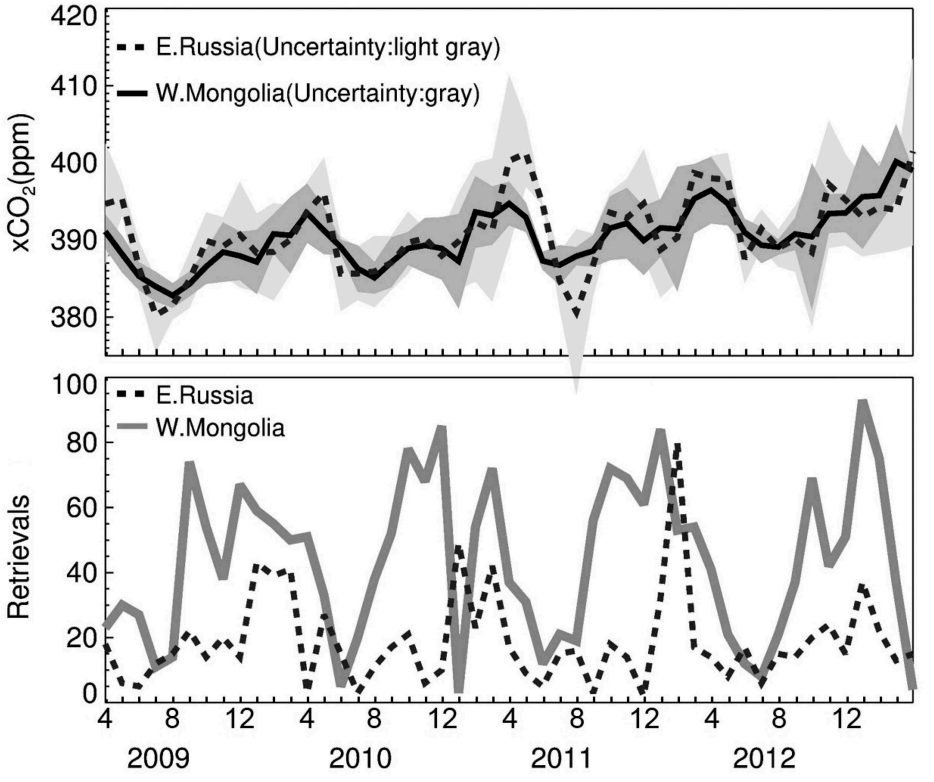

Figure 5. The monthly mean XCO_2 over western Mongolia (black solid line) and far eastern Russia (black dashed line) from April 2009 to April 2013 (top panel) and the total number of monthly 'good' retrievals over the regions (bottom panel).

The overall GOSAT XCO_2 values at SMA, GYG, SCH were +6.9, +5.6, and +9.9 ppm, respectively, compared to the background region (values in the parenthesis in Table 1). Considering the overall monthly mean variability of the background region (± 3.2 ppm), these enhancements are significant. If we include only the cold season data, the XCO_2 enhancement is larger (SMA: +7.9 ppm, GYG: +7.2 ppm, and SCH: +10.6 ppm), reflecting higher energy consumption for heating by urban households (SMA) and power plants (GYG, SCH) during the cold season (Mo 2012).

Another reason for larger XCO_2 enhancements over Korean footprints than over the Los Angeles Basin (about 3.2 ppm by Kort et al. (2012)) is the large-scale and persistent impact of transboundary CO_2 plumes from China, which likely contribute to the absolute value of the XCO_2 enhancements.

Figure 7 shows the back trajectories of continental outflow from China toward GYG and SCH during the cold season from 2010 to 2013. Backward trajectories arriving at 1500 m a.s.l. every 00:00, 06:00, 12:00, and 18:00 UTC (03:00, 09:00, 18:00, and 21:00 local time) were calculated using the National Oceanic and Atmospheric Administration (NOAA) Air Resources Laboratory (ARL) Hybrid Single-Particle Lagrangian Integrated Trajectory (HYSPLIT) model (version 4) (Rolph 2017; Stein et al. 2015). The 48 h back trajectories indicate that CO_2 is transported mainly from northeastern China, in the

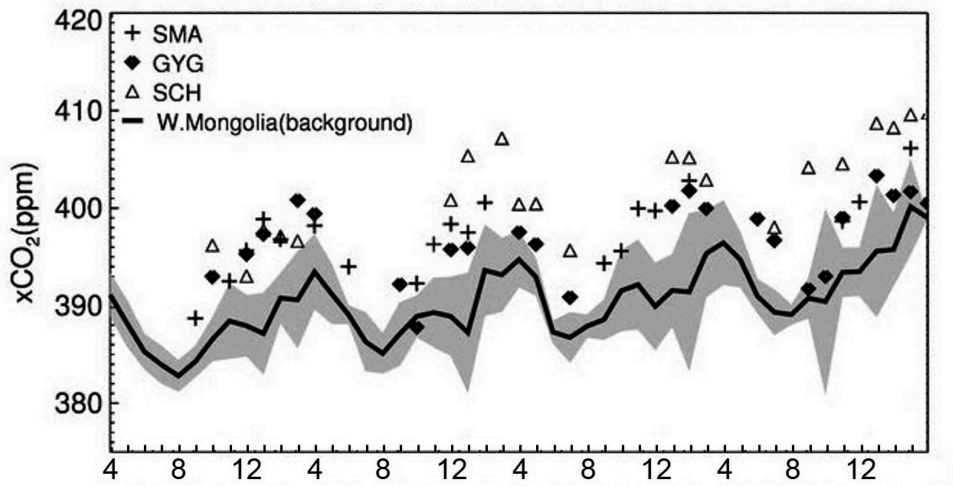

Figure 6. The monthly XCO_2 of the three GOSAT footprints of South Korea (SMA, GYG, SCH) above that of western Mongolia (black solid line).

Table 1. XCO_2 enhancements and emission intensities over the three-GOSAT footprints (SMA, GYG, SCH). Net enhancement indicates that the XCO_2 enhancement excluded the contribution by latitudinal gradient, Chinese CO_2 emissions, and differences in biogenic fluxes (described in section 3–2). The values in the parenthesis indicate the estimates from all cases (all seasons).

ACOS GOSAT	SMA	GYG	SCH
Retrieval numbers	14(20)	11(24)	12(22)
Enhancements(ppm)	7.9 ± 2.3(6.9)	7.3 ± 2.5(5.6)	10.7 ± 3.6(9.9)
Net enhancement(ppm)	4.8 ± 3.1	4.2 ± 3.2	7.6 ± 4.1
Trend (ppm $year^{-1}$)	+ 0.4(0.4)	−0.2(−0.9)	+ 1.3(1.4)
FFDAS (kg m^{-2} $year^{-1}$)	140	308	270

region between Shandong and Liaoning (Figure 7). The influence of continental outflow is also supported by the average wind directions (0.5° × 0.5° at 850 hPa) over East Asia during the cold season (November–February) between 2009 and 2013 (Figure 8), which were analysed by the Global Forecast System (GFS) from historical Unidata internet data distribution (IDD) (Unidata/NCAR/NWS/NOAA/USDC/ECMWF 2003). These wind directions suggest that CO_2 emissions over northeastern China largely affected XCO_2 over South Korea.

We calculated the impact of Chinese emissions on XCO_2 over South Korea using GEOS-Chem, a chemical transport model (v9-01–03). The CO_2 simulation model was developed by Nassar et al. (2010) using a fossil fuel emission inventory produced by the Carbon Dioxide Information and Analysis Centre (CDIAC) (Andres et al. 2011). We tagged CO_2 concentration produced only by fossil fuel combustion (CO_{2ff}) and calculated its aggregated contribution to XCO_2 (XCO_{2ff}) from 2009 to 2010, using the model settings described by Shim, Lee, and Wang (2013) with a 2.0 × 2.5° horizontal resolution. We assumed that the discrepancy between the monthly XCO_{2ff} enhancement (in comparison with western Mongolia) over South Korea and that over the adjacent Yellow Sea (grey region in Figure 4) (ΔXCO_{2ff}(S. Korea) – ΔXCO_{2ff}(Yellow Sea)) during the cold season could roughly represent the background

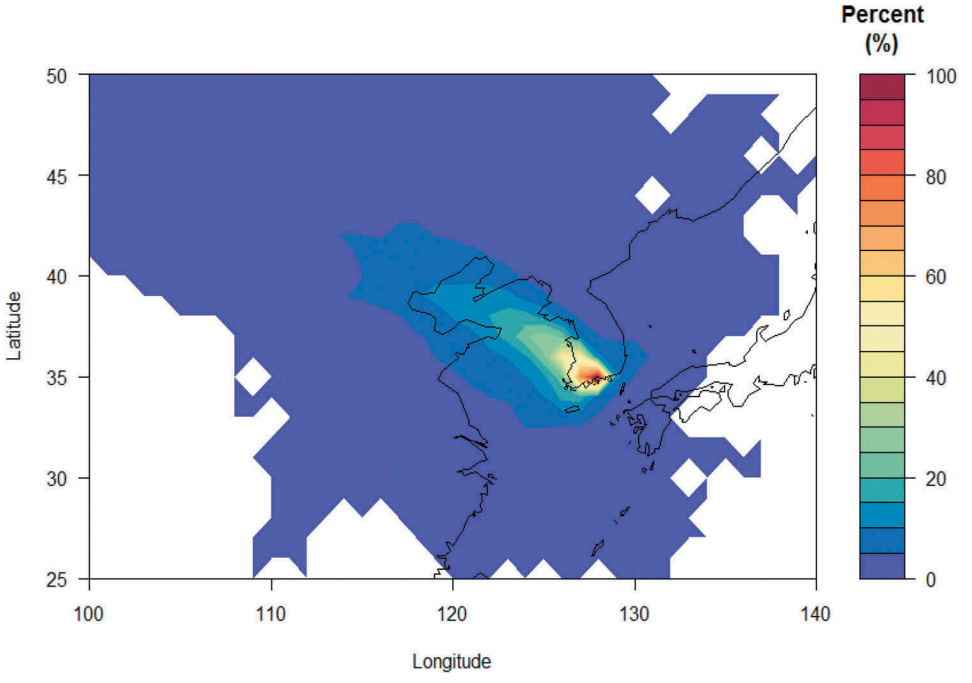

Figure 7.. 48 hours backtrajectory analysis for GYG & SCH (brown dot in the southern coast of the Korean Peninsula) during 2009–2013. The colour denotes per cent (%) of the total counts of the trajectories passed over each hexagonal grid. The trajectories represented only for the cold season (November–February).

XCO_2 enhancement from Chinese fossil fuel combustion, which is about 1.5 ± 0.2 ppm. The GEOS-Chem adjoint sensitivity test for the source-receptor relation of XCO_2 by Liu et al. (2015a) showed that XCO_2 signals in the winter are more associated with the local (or regional) contributions over East Asia. The possibility of additional contribution to XCO_2 by vegetation uptake between South Korea and western Mongolia is small: 0.26 ± 0.7 ppm.

As stated in Section 3–1, the contribution to XCO_2 due to the latitudinal difference between the western Mongolia and Korean GOSAT footprints is about 1.3 ppm. When we consider the additional contribution by Chinese fossil fuel combustion (about 1.5 ppm) and biogenic influence (about 0.3 ppm), the net XCO_2 enhancements by local emissions at SMA, GYG, and SCH would be 4.8 ± 3.1 ppm, 4.2 ± 3.2 ppm, and 7.6 ± 4.1 ppm, respectively.

Interestingly, although the distance between the GYG and SCH footprints is only 26.2 km, the XCO_2 enhancement over SCH (7.6 ± 4.1 ppm) was significantly higher than that over GYG (4.2 ± 3.2 ppm (*t*-test: $p = 0.002$)) with lower residual standard error of linear regressions (3.6 (SCH) and 3.1 (GYG)) than standard deviation (4.1 (SCH) and 3.2 (GYG)). That indicates the data from these two GOSAT XCO_2 footprints are separable, which is also supported by a different 4-year trend in these XCO_2 enhancements (GYG: –0.2 ppm $year^{-1}$ ($p = 0.142$) and SCH: +1.3 ppm $year^{-1}$ ($p = 0.020$), respectively) (Table 1 and Figure 9).

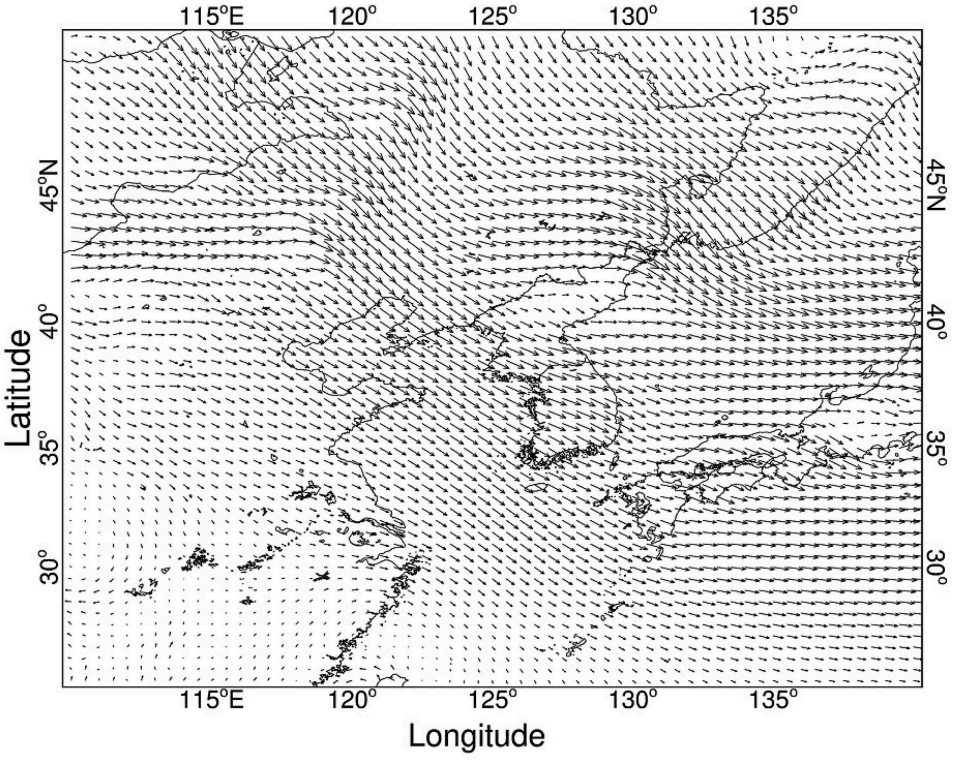

Figure 8. Average wind directions (0.5°□0.5° at 850 hPa) over East Asia during the cold season (November–February, 2009–2013). The analysis data are from the Global Forecast System (GFS) analysis field (http://rda.ucar.edu/datasets/ds335.0/).

The 4.2–7.6 ppm net enhancement over South Korean footprints was higher than that of the Los Angeles Basin (+3.2 ppm, Kort et al. 2012; 2–8 ppm, Wunch et al. 2011) and that of East Asian cities (0.6–3.3 ppm, Janardanan et al. 2016). One reason for the higher enhancement observed over Korea is that XCO_2 enhancements over Korea are based on a single XCO_2 footprint over large local sources, not an average over a larger urban area such as the Los Angeles Basin, suggesting that the XCO_2 over Korean footprints likely reflects specific local emission intensity (i.e., kg m^{-2}) rather than total CO_2 emissions over the specific area. The average CO_2 emission intensity over the SMA footprint based on the Fossil Fuel Data Assimilation System (FFDAS v2.0) (0.1 × 0.1° in scale) was 140 kg m^{-2} $year^{-1}$, whereas the mean emission intensity over the entire Los Angeles Basin was 49 kg m^{-2} $year^{-1}$ (Brioude et al. 2013). However, the larger net XCO_2 enhancement over SCH (7.6 ppm) compared with that over GYG (4.2 ppm) cannot be explained by FFDAS emission intensity (270 kg m^{-2} $year^{-1}$ for SCH and 308 kg m^{-2} $year^{-1}$ for GYG), possibly reflecting uncertainties in the emission estimates, since there are no other large emission sources nearby.

To investigate the impact of local emissions on GOSAT XCO_2, we analysed data from the national bottom-up greenhouse gas emissions inventory (GHG-CAPSS 2016), which was recently constructed by the Korean Ministry of Environment (KMOE). The GHG-CAPSS inventory was estimated based on IPCC guidelines for national greenhouse gas

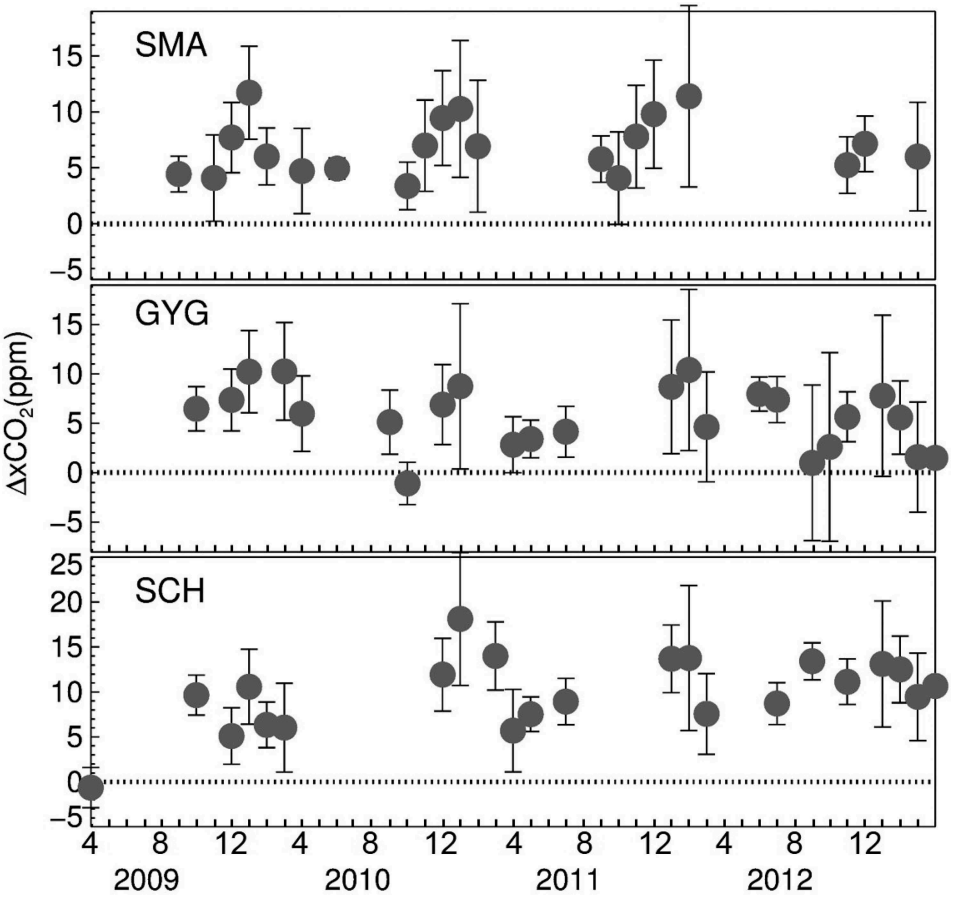

Figure 9. Same as Figure 6, but for XCO_2 enhancements of SMA, GYG, and SCH above western Mongolia.

inventories (2018), and provides annual total GHG emissions for individual local administrative districts (about 250) from 2010 to 2013.

The annual emission intensity over the SMA footprint (Sungbuk-ku, located in north-central Seoul (Figure 3)), based on GHG-CAPSS, is about 36 kg m^{-2} $year^{-1}$, which is comparable to that of the entire Seoul area (30–40 kg m^{-2} $year^{-1}$). The estimate of annual total CO_2 emissions over Seoul (2×10^{10}–2.5×10^{10} kg $year^{-1}$) is similar to that of the Hadong coal power plants (about 2.5×10^{10} kg $year^{-1}$). Considering the similar net XCO_2 enhancement produced by SMA and GYG (4.8 vs. 4.2 ppm, respectively), emissions from the adjacent Gwangyang Steelworks (about 4×10^{10} kg $year^{-1}$) may not be a critical contribution to GYG XCO_2 enhancement. The large difference in emission intensity in the SMA footprint (under Sungbuk-ku, in Seoul) between GHG-CAPSS (about 36 kg m^{-2} $year^{-1}$) and FFDAS (about 140 kg m^{-2} $year^{-1}$) reflects large uncertainties in the emissions estimates. The direct comparison between FFDAS and GHG-CAPSS is difficult because FFDAS has gridded data and GHG-CAPSS has total emissions for the individual administrative district. Moreover, FFDAS data were estimated based on the nighttime lights and population, which could lead to biases in emissions in some cases such as dark emissions or lower population on a finer

spatial scale (Oda and Maksyutov 2011; Asefi-Najafabady et al. 2014). Discussion of the GYG and SCH emissions intensity is not possible using GHG-CAPSS because the annual emissions represent the total emissions over the entire area of the local administrative district (500–700 km^2) even though the targeted point sources (Gwangyang Steelwork, Hadong and Samcheonpo power plants) are responsible for most of the total emissions from the local administrative districts (>80% of CO_2 emissions, National Institute of Environmental Research (NIER) of Korea 2016).

To evaluate the consistency between observed enhancements and the reported bottom-up emissions, we simply estimated enhanced XCO_2 for each GOSAT footprint created by the local emissions (GHG-CAPSS) from GYG (Hadong power plants only) and SCH (Samcheonpo power plants). The assumption is that the emitted CO_2 travels and mixes vertically within the total GOSAT column (diameter of about 10.5 km) at the average local wind speed (2.5 ms^{-1}, mean residence time of about 1.2 h in the GOSAT footprint). This estimation procedure has been described by NRC (2010), and the contributions to the GOSAT XCO_2 enhancements by emissions from GYG and SCH are approximately 3.0 and 2.6 ppm, respectively. We did not estimate ΔXCO_2 for the SMA footprint because SMA is not a unique point source; rather, it is widely affected by all of Seoul as well as adjacent emissions. A general order-of-magnitude comparison of these estimates of observed GOSAT XCO_2 enhancements lends confidence to our procedure for identifying anthropogenically influenced XCO_2 enhancement. However, the smaller magnitude of these bottom-up estimates compared to observed GOSAT XCO_2 enhancements (2.6–3.0 ppm vs. 4.2–7.6 ppm) implies that there are large uncertainties (e.g., double) in some parts of the bottom-up emissions inventory (GHG-CAPSS). This possibility is supported by the fact that two of the six coal power plants at SCH had no emission abatement facilities; yet, the same emission coefficients have been applied to estimate the GHG-CAPSS inventory, which only considered the general emission coefficient and energy use instead of accurate measurements of emissions fluxes (Koo 2016). The results of coal burning at SCH without emission abatement facilities made SCH the top-ranked pollutant-emitting plants in South Korea (Kim 2017), strongly suggesting that CO_2 emissions from the Samcheonpo coal-power plants (SCH) have been underestimated (T. Yoon, personal communication, 2017).

Other possible contributions to the observed ΔXCO_2 include the impact of a broader set of regional emissions, i.e., other domestic emissions.

As described above, the separate XCO_2 trends for GYG (–0.2 ppm $year^{-1}$) and SCH (+1.3 ppm $year^{-1}$) were compared with the GHG-CAPSS inventory from 2010 to 2013. There were slightly different annual emission trends between Hadong (–470 kg $year^{-1}$; GYG) and Samcheonpo (+ 250 kg $year^{-1}$); however, they were likely too small to explain the XCO_2 differences estimated for the Los Angeles Basin (Kort et al. 2012). These comparisons suggest that more accurate emission estimates using emissions intensity information (i.e., gridded data) based on local validation of GOSAT XCO_2 with ground and aircraft measurements near/over the emission sources are required.

4. Conclusions and discussions

We used 4-year GOSAT XCO_2 data (2010–2013) to identify the impacts of large urban/local anthropogenic CO_2 emissions over South Korea. Satellite XCO_2 observations over

East Asia are limited by high, persistent, and extensive aerosol pollution and intensive cloud cover, particularly during the wet season, which often reduces the amount of reliable retrievals for analysis. Due to the significant reduction in GOSAT retrievals during the monsoon season and dominant downwind effects with high aerosol loading in the spring and fall, we found that the cold season (November–February) was the most appropriate period in which to analyse XCO_2 enhancements over East Asia.

Determining a relatively 'clean' background region for estimating XCO_2 enhancements over large emission sources is an important step in using remote sensing data to detect local enhancements of XCO_2 over Korean large point sources. Because no major emission sources had stable seasonal variation, we selected XCO_2 over western Mongolia (upwind region over 95°E – 105°E, 44°N – 49°N) as a background for East Asia.

We focused on three local GOSAT XCO_2 footprints with the highest retrieval frequency in South Korea: the Seoul Metropolitan Area (SMA), the Gwangyang Steelworks and Hadong power plants (GYG), and the Samcheonpo power plants (SCH). The range of consistent XCO_2 enhancements was 7.3–10.7 ppm; we estimated the net XCO_2 enhancement by subtracting the latitudinal gradient (1.3 ppm), Chinese emission contribution (1.5 ppm), and differences in biogenic fluxes (0.3 ppm) calculated by GEOS-Chem CO_2 simulations, resulting in net ΔXCO_2 values of 4.8 ppm (SMA), 4.2 (GYG), and 7.6 (SCH). The net XCO_2 enhancements were higher than previous estimates for the Los Angeles Basin (Kort et al. 2012). Such higher enhancements may represent higher emission intensities from large point sources over the individual GOSAT footprint, rather than larger urban-scale emissions. In particular, differences in net XCO_2 enhancements and trends between GYG (+4.2 ppm, –0.2 ppm $year^{-1}$) and SCH (+7.6 ppm, +1.3 ppm $year^{-1}$) indicate that these closely located XCO_2 footprints (about 26 km apart) are separable, suggesting that GOSAT XCO_2 can capture the impact of large individual point sources. These findings are important for inferring local CO_2 emissions with remote sensing data because the separable and consistent enhancements of GOSAT XCO_2 can provide additional constraints on local-scale emissions under the restricted conditions for satellite data sampling over the polluted, downwind regions of East Asia. Such enhanced XCO_2 signals can constrain current uncertain estimates of local anthropogenic sources made using fine-scale inverse modelling techniques. Mismatches between XCO_2 enhancements of the Korean footprints and the corresponding bottom-up emissions inventory imply great uncertainty in some parts of urban/local scale emissions estimates Table 2.

Despite these findings for satellite footprints, limitations remain in verifying and estimating local CO_2 emissions, necessitating further research efforts to reduce these

Table 2. The national CO_2 emission estimates over the three GOSAT footprints. The value of SMA in 2010 indicate the emission estimate above the GOSAT footprint (near Sungbuk-ku). The values in the parentheses of SMA in 2010 indicate the emission estimates above entire Seoul.

National emissions (GHG-CAPSS, kg CO_2 $year^{-1}$)	SMA	GYG (Gwangyang & Hadong)	SCH
2010	880,129,000 (23,029,962,000)	30,530,895,000(Hadong) 36,575,675,000 (Gywanyang)	25,646,083,000
2011	905,225,000 (26,118,383,000)	31,199,196,000 46,353,778,000	26,285,155,000
2012	893,142,000 (24,978,725,000)	31,003,896,000 45,290,259,000	30,207,382,000
2013	915,357,000 (25,119,693,000)	30,476,961,000 42,484,896,000	26,483,652,000

uncertainties. First, the impact of long-range CO_2 transport (i.e., plumes from China) and the influence of the latitudinal gradient in XCO_2 has been estimated; however, coarse model resolution, uncertain emission inventories, and highly variable latitudinal gradients increase estimation uncertainties. Second, consistent and intensive measurements are necessary to validate local XCO_2 concentrations and verify urban-scale emission estimates. The intensive measurement campaign over the Los Angeles Basin and Central Valley (CalNex campaign, Ryerson et al. 2013) serves as a good example. Lastly, Korean GHG emissions are not estimated based only on nationwide monitoring systems and emission fluxes, but also on regulatory documentation for the national environmental impact assessment, which is required for major emitting facilities before they are permitted to operate in Korea. However, no legally binding verification of large emissions is conducted after operation, which may also contribute to uncertainties in emissions estimates in South Korea. The possible underestimation of emissions from plants without emission abatement facilities at the Samcheonpo coal power plants is a good example. Reinforcing environmental impact assessments with consistent measurements and verifications for large emission sources in Korea is critical to managing the national carbon reduction target and reducing the large uncertainties in emission estimates.

Acknowledgments

This work was jointly supported by the Korea Meteorological Administration Research and Development Program under Grant KMIPA (No. 2015-2022) and by the National Strategic Project-Fine particle of the National Research Foundation of Korea (NRF) funded by the Ministry of Science and ICT (MSIT), the Ministry of Environment (ME), and the Ministry of Health and Welfare (MOHW) (No. 2017M3D8A1092026). C. Shim thanks Korea Environment Institute (KEI) for the institutional support. These data were produced by the ACOS/OCO-2 project at the Jet Propulsion Laboratory, California Institute of Technology, and obtained from the ACOS/OCO-2 data archive maintained at the NASA Goddard Earth Science Data and Information Services Center. DKH recognizes support from NOAA NA14OAR4310136.

Disclosure statement

No potential conflict of interest was reported by the authors.

Funding

This work was supported by the National Oceanic and Atmospheric Administration [NA14OAR4310136];National Research Foundation of Korea [2017M3D8A1092026];Korea Meteorological Administration Research and Development Program [KMIPA 2015-2022].

ORCID

Changsub Shim http://orcid.org/0000-0003-1735-6655

References

Andres, R. J., J. S. Gregg, L. Losey, G. Marland, and T.A. Boden. 2011. Monthly, Global Emissions of Carbon dioxide from Fossil Fuel consumption. *Tellus*, 63B: 309-327, doi:10.1111/j.1600-0889.

Asefi-Najafabady, S., P. J. Rayner, K. R. Gurney, A. McRobert, Y. Song, K. Coltin, J. Huang, C. Elvidge, and K. Baugh. 2014. "A Multiyear, Global Gridded Fossil Fuel CO_2 Emission Data Product: Evaluation and Analysis of Results." *Journal of Geophysical Research: Atmospheres* 119. doi:10.1002/2013JD021296.

Boden, T. A., G. Marland, and R. J. Andres. 2010. *Global, Regional, and National Fossil-Fuel CO_2 Emissions*. Oak Ridge, Tenn., U.S.A.: Carbon Dioxide Information Analysis Center, Oak Ridge National Laboratory, U.S. Department of Energy. doi:10.3334/CDIAC/00001_V2010.

Bovensmann, H., J. P. Burrows, M. Buchwitz, J. Frerick, S. No¨El, V. V. Rozanov, K. V. Chance, and A. Goede. 1999. "SCIAMACHY –Mission Objectives and Measurement Modes." *Journal of the Atmospheric Sciences* 56: 127–150. doi:10.1175/1520-0469(1999)056<0127:SMOAMM>2.0.CO;2.

Brioude, J., W. M. Angevine, R. Ahmadov, S.-W. Kim, S. Evan, S. A. McKeen, E.-Y. Hsie, et al. 2013. "Top-Down Estimate of Surface Flux in the Los Angeles Basin Using a Mesoscale Inverse Modeling Technique: Assessing Anthropogenic Emissions of CO, NO_x, and CO_2 and Their Impacts." *Atmospheric Chemistry and Physics* 13 :3661–3677. doi:10.5194/acp-13-3661-2013.

Burrows, J. P., E. H¨Olzle, A. P. H. Goede, H. Visser, and W. Fricke. 1995. "SCIAMACHY – Scanning Imaging Absorption Spectrometer for Atmospheric Chartography." *Acta Astronautica* 35 (7): 445–451. doi:10.1016/0094-5765(94)00278-T.

Chevallier, F., P. I. Palmer, L. Feng, H. Boesch, C. W. O'Dell, and P. Bousquet. 2014. "Toward Robust and Consistent Regional CO_2 Flux Estimates from in Situ and Spaceborne Measurements of Atmospheric CO_2." *Geophysical Research Letters* 41 (3): 1065–1070. doi:10.1002/2013GL058772.

Chevallier, F., R. J. Engelen, and P. Peylin. 2005. "The Contribution of AIRS Data to the Estimation of CO_2 sources and sinks." *Geophysical Research Letters* 32: L23801, doi: 10.1029/2005GL024229.

Ciais, P., D. Crisp, H. D. van der Gon, R. Engelen, G. Janssens-Maenhout, M. Heimann, P., Rayner, and M. Scholze. 2015. "Towards a European Operational Observing System to Monitor Fossil Fuel CO_2 Emissions." In *European Commission*. Accessed 26 July 2018. www.copernicus.eu/main/towards-european-operational-observing-system-monitor-fossil-co2-emissions

Ciais, P., P. J. Rayner, F. Chevallier, P. Bousquet, M. Logan, P. Peylin, and M. Ramonet. 2010. "Atmospheric Inversions for Estimating CO_2 Fluxes: Methods and Perspectives." *Climate Change* 103: 69–92. doi:10.1007/s10584-010-9909-3.

Crevoisier, C., A. Ch´Edin, H. Matsueda, T. Machida, R. Armante, and N. A. Scott. 2009. "First Year of Upper Tropospheric Integrated Content of CO_2 from IASI Hyperspectral Infrared Observations." *Atmospheric Chemistry and Physics* 9: 4797–4810. doi:10.5194/acp-9-4797-2009.

Crisp, D., B. M. Fisher, C. O'Dell, C. Frankenberg, R. Basilio, H. Bösch, L. R. Brown, et al. 2012. "The ACOS CO_2 Retrieval Algorithm – Part II: Global XCO_2 Data Characterization." *Atmospheric Measurement Techniques* 5 :687–707. doi:10.5194/amt-5-687-2012.

Crisp, D., R. M. Atlas, F.-M. Br´Eon, L. R. Brown, J. P. Burrows, P. Ciais, B. J. Connor, et al. 2004. "The Orbiting Carbon Observatory (OCO) Mission." *Advances in Space Research* 34 :700–709. doi:10.1016/j.asr.2003.08.062.

Deng, F., D. B. A. Jones, C. W. O'Dell, R. Nassar, and N. C. Parazoo. 2015. "Combining GOSAT xCO_2 Observations over Land and Ocean to Improve Regional CO_2 Flux Estimates." *Journal of Geophysical Research: Atmospheres* 121: 1896–1913. doi:10.1002/2015JD024157.

Deng, F., D. B. A. Jones, D. K. Henze, N. Bousserez, K. W. Bowman, J. B. Fisher, R. Nassar, et al. 2014. "Inferring Regional Sourecs and Sinks of Atmospheric CO_2 from GOSAT xCO_2 Data." *Atmospheric Chemistry and Physics* 14 (7): 3703–3727. doi:10.5194/acp-14-3703-2014.

Eldering, A., C. W. O'Dell, P. O. Wennberg, D. Crisp, M. R. Gunson, C. Viatte, C. Avis, et al. 2017. "The Orbiting Carbon Observatory-2: First 18 Months of Science Data Products." *Atmospheric Measurement Techniques* 10 :549–563. doi:10.5194/amt-10-549-2017.

Engelen, R. J., and G. L. Stephens. 2004. "Information Content of Infrared Satellite Sounding Measurements with respect to CO_2." *Journal of Applied Meteorology and Climatology* 43: 373–378. doi:10.1175/1520-0450(2004)043<0373:ICOISS>2.0.CO;2.

GEOS-Chem Model, Version 9-01-03. Accessed 20 July 2018. http://www.geos-chem.org
Guan, D., Z. Liu, Y. Geng, S. Lindner, and K. Hubacek. 2012. "The Gigatonne Gap in China's Carbon Dioxide Inventories." *Nature Climate Change* 2: 672–675. doi:10.1038/nclimate1560.
IPCC. 2014. *Climate Change 2014: Synthesis Report Summary for Policymakers to the Fifth Assessment Report of the Intergovernmental Panel on Climate Change*, 32. Geneva, Switzerland: IPCC. Accessed 26 July 2018. www.ipcc.ch/report/ar5/syr/
IPCC guidelines for national greenhouse gas inventories. 2018. Accessed 26 July 2018.www.ipcc-nggip.iges.or.jp/public/gl/invs1.html
Janardanan, R., S. Maksyutov, T. Oda, M. Saito, J. W. Kaiser, A. Ganshin, A. Stohl, T. Matsunaga, Y. Yoshida, and T. Yokota. 2016. "Comparing GOSAT Observations of Localized CO_2 Enhancements by Large Emitters with Inventory-Based Estimates." *Geophysical Research Letters* 43: 3486–3493. doi:10.1002/2016GL067843.
Kadygrov, N., S. Maksyutov, N. Eguchi, T. Aoki, T. Nakazawa, T. Yokota, and G. Inoue. 2009. "Role of Simulated GOSAT Total Column CO_2 Observations in Surface CO_2 Flux Uncertainty Reduction." *Journal of Geophysical Research* 114: D21208. doi:10.1029/2008JD011597.
Keppel-Aleks, G., P. O. Wennberg, C. W. O'Dell, and D. Wunch. 2013. "Towards Constraints on Fossil Fuel Emissions from Total Column Carbon Dioxide." *Atmospheric Chemistry and Physics* 13: 4349–4357. doi:10.5194/acp-13-4349-2013.
Keppel-Aleks, G., P. O. Wennberg, and T. Schneider. 2011. "Sources of Variations in Total Column Carbon Dioxide." *Atmospheric Chemistry and Physics* 11: 3581–3593. doi:10.5194/acp-11-3581-2011.
Kim, D. 2017. "Nam-Hae Local Government Is Trying to Assess the Environment Impact by near Coal Power Plants." *Pressian*. Accessed 20 November 2017. (in Korean). www.pressian.com/news/article.html?no=156781
Kim, Y. 2016. "A Report of Gwangyang Steelworks." *Yeon Hap News*. Accessed 09 February 2017. (in Korean). www.yonhapnews.co.kr/bulletin/2016/04/15/0200000000AKR20160415138900003.HTML
Koo, K. 2016. "Citizen's Environment Research Center Said the Environment Assessment Reports of Domestic Power Plants are Nonsense." *Gyungnam citizen's news*. Accessed 10 November 2017. (in Korean). www.gndomin.com/news/articleView.html?idxno=124292
Korea South-East Power Cooperation (KOEN). 2016. Accessed 9 February 2017. (In Korean). Operation Information Retrieved from www.kosep.co.kr:8100/kosep/br/sp/main.do?menuCd=BR0101
Korea Southern Power Cooperation (KOSPO). 2016. Accessed 9 February 2017. (In Korean). Operational information retrieved from www.kospo.co.kr/?mn=sub&mcode=06040300
Kort, E. A., C. Frankenberg, C. E. Miller, and T. Oda. 2012. "Space-Based Observations of Megacity Carbon Dioxide." *Geophysical Research Letters* 39: L17806. doi:10.1029/2012GL052738.
Kulawik, S. S., D. B. A. Jones, R. Nassar, F. W. Irion, J. R. Worden, K. W. Bowman, T. Machida, et al. 2010. "Characterization of Tropospheric Emission Spectrometer (TES) CO_2 for Carbon Cycle Science." *Atmospheric Chemistry and Physics* 10 :5601–5623. doi:10.5194/acp-10-5601-2010.
Kuze, A., H. Suto, M. Nakajima, and T. Hamazaki. 2009. "Thermal and near Infrared Sensor for Carbon Observation Fourier-Transform Spectrometer on the Greenhouse Gases Observing Satellite for Greenhouse Gases Monitoring." *Applied Optics* 48 (35): 6716–6733. doi:10.1364/AO.48.006716.
Liu, J., K. W. Bowman, and D. K. Henze. 2015a. "Source-Receptor Relationships of Column-Average CO_2 and Implications for the Impact of Observations on flux Inversions." *Journal of Geophysical Research: Atmospheres* 120: 5214–5236. doi:10.1002/2014JD022914.
Liu, J., K. W. Bowman, M. Lee, D. K. Henze, N. Bousserez, H. Brix, G. J. Collatz, et al. 2014. "Carbon Monitoring System Flux Estimation and Attribution: Impact of ACOS-GOSAT XCO_2 Sampling on the Inference of Terrestrial Biospheric Sources and Sinks." *Tellus B: Chemical and Physical Meteorology* 66 :22486. doi:10.3402/tellusb.v66.22486.
Liu, Z., D. Guan, W. Wei, S. J. Davis, P. Ciais, J. Bai, S. Peng, et al. 2015b. "Reduced Carbon Emission Estimates from Fossil Fuel Combustions and Cement Production in China." *Nature* 524 :335–338. doi:10.1038/nature14677.

Mo, J. 2012. "Estimating Hourly National Electricity Demand for Management of Domestic Electric Vehicles and Policy Implication." Issue paper of Korea Institute for Industrial Economics and Trade (KIET 2012-294). (in Korean)

Nassar, R., D. B. A. Jones, P. Suntharalingam, J. M. Chen, R. J. Andres, K. J. Wecht, R. M. Yantosca, S. S. Kulawik, K.W. Bowman, J.R. Worden, T. Machida, and H. Matueda. 2010. "Modeling Global Atmospheric CO_2 with Improved Emission Inventories and CO_2 Production from the Oxidation of Other Carbon Species." *Geosci. Mode Dev*, 3: 689-716, 2010 www.geosci-model-dev.net/3/689/2010/ doi:10.5194/gmd-3-689-2010.

National Aeronautics and Space Administration (NASA). 2018. Goddard Earth Science Data and Information Services Center. Accessed 20 July 2018. http://disc.sci.gsfc.nasa.gov/acdisc/data-holdings/acos-data-holdings

National Institute of Environmental Research (NIER) of Korea. 2016. *Greenhouse gases-Clean Air Policy Support System (GHG-CAPSS) Emissions Inventory and Methodological Guide*. Incheon: NEIR. (in Korean).

National Research Council (NRC). 2010. *Verifying Greenhouse Gas Emissions: Methods to Support International Climate Agreements*. Washington, DC: The National Academies Press. doi:10.17226/12883.

Newman, S., S. Jeong, M. L. Fischer, X. Xu, C. L. Haman, B. Lefer, and S. Alvarez. 2013. "Diurnal Tracking of Anthropogenic CO_2 Emissions in the Los Angeles Basin Megacity during Spring 2010." *Atmospheric Chemistry and Physics* 13: 4359–4372. doi:10.5194/acp-13-4359-2013.

O'Dell, C. W., B. Connor, H. Bösch, D. O'Brien, C. Frankenberg, R. Castano, M. Christi, et al. 2012. "The ACOS CO_2 Retreival Algorithm – Part 1: Description and Validation against Synthetic Observations." *Atmospheric Measurement Techniques* 5 :99–121. doi:10.5194/amt-5-99-2012.

Oda, T., and S. Maksyutov. 2011. "Very High-Resolution (1 Km × 1 Km) Global Fossil Fuel CO_2 Emission Inventory Derived Using a Point Source Database and Satellite Observations of Nighttime Lights."." *Atmospheric Chemistry and Physics* 11: 543–556. doi:10.5194/acp-11-543-2011.

Pataki, D. E., T. Xu, Y. Q. Luo, and J. R. Ehleringer. 2007. "Inferring Biogenic and Anthropogenic Carbon Dioxide Sources across an Urban to Rural Gradient." *Oecologia* 152 (2): 307–322. doi:10.1007/s00442-006-0656-0.

Reuter, M., M. Buchwitz, M. Hilker, J. Heymann, O. Schneising, D. Pillai, H. Bovensmann, et al. 2014. "Satellite-Inferred European Carbon Sink Larger than Expected." *Atmospheric Chemistry and Physics* 14 :13739–13753. doi:10.5194/acp-14-13739-2014.

Rigby, M., R. Toumi, R. Fisher, D. Lowry, and E. G. Nisbet. 2008. "First Continuous Measurements of CO_2 Mixing Ratio in Central London Using a Compact Diffusion Probe." *Atmospheric Environment* 42 (39): 8943–8953. doi:10.1016/j.atmosenv.2008.06.040.

Rolph, G. D. 2017. *Real-Time Environmental Applications and Display sYstem (READY) Website*. College Park, MD: NOAA Air Resources Laboratory. Accessed 20 July 2018. www.ready.noaa.gov

Ryerson, T. B., A. E. Andrews, W. M. Angevine, T. S. Bates, C. A. Brock, B. Cairns, R. C. Cohen, et al. 2013. "The 2010 California Research at the Nexus of Air Quality and Climate Change (Calnex) Field Study." *Journal of Geophysical Research: Atmospheres* 118 :5830–5866. doi:10.1002/jgrd.50331.

Shim, C., J. Lee, and Y. Wang. 2013. "Effect of Continental Sources and Sinks on the Seasonal and Latitudinal Gradient of Atmospheric Carbon Dioxide over East Asia." *Atmospheric Environment* 79: 853–860. doi:10.1016/j.atmosenv.2013.07.055.

Stein, A. F., R. R. Draxler, G. D. Rolph, B. J. B. Stunder, M. D. Cohen, and F. Ngan. 2015. "NOAA's HYSPLIT Atmospheric Transport and Dispersion Modeling System." *Bulletin of the American Meteorological Society* 96: 2059–2077. doi:10.1175/BAMS-D-14-00110.1.

Unidata/University Corporation for Atmospheric Research, National Centers for Environmental Prediction/National Weather Service/NOAA/U.S. Department of Commerce, and European Centre for Medium-Range Weather Forecasts. 2003. updated daily. "Historical Unidata Internet Data Distribution (IDD) Gridded Model Data." *Research Data Archive at the National Center for Atmospheric Research, Computational and Information Systems Laboratory*. Accessed 25 February 2017. rda.ucar.edu/datasets/ds335.0/

Wunch, D., P. O. Wennberg, G. C. Toon, B. J. Connor, B. Fisher, G. B. Osterman, and C. Frankenberg. 2011. "A Method for Evaluating Bias in Global Measurements of CO_2 Total Columns from Space." *Atmospheric Chemistry and Physics* 11: 12317–12337. doi:10.5194/acp-11-12317-2011.

Yokota, T., Y. Yoshida, N. Eguchi, Y. Ota, T. Tanaka, H. Watanabe, and S. Maksyutov. 2009. "Global Concentration of CO_2 and CH_4 Retrieved from GOSAT: First Preliminary Results." *Scientific Online Letters on the Atmosphere (SOLA)* 5: 160–163. doi:10.2151/sola.2009-041.

Zhang, L., H. Jiang, and X. Zhang. 2015. "Comparison Analysis of the Global Carbon Dioxide Concentration Column Derived from SCIAMACHY, AIRS, and GOSAT with Surface Station Measurements." *International Journal of Remote Sensing* 36 (5): 1406–1423. doi:10.1080/01431161.2015.1009656.

Zhou, M., B. Dils, P. Wang, R. Detmers, Y. Yoshida, C. W. O'Dell, D. G. Feist, et al. 2016. "Validation of TANSO-FTS/GOSAT XCO_2 and XCH_4 Glint Mode Retrievals Using TCCON Data from Near-Ocean Sites." *Atmospheric Measurement Techniques* 9 (3): 1415–1430. doi:10.5194/amt-9-1415-2016.